J|A|C|S
ARTICLES
Published on Web 10/05/2002

The Interplay of Bent-Shape, Lateral Dipole and Chirality in Thiophene Based Di-, Tri-, and Tetracatenar Liquid Crystals

S. Holger Eichhorn, Alexander J. Paraskos, Keiki Kishikawa, and Timothy M. Swager*

Contribution from the Department of Chemistry and Center for Materials Science and Engineering, Massachusetts Institute of Technology, Cambridge, Massachusetts 02139

Received May 6, 2002

Abstract: A range of mesogenic molecules varying in both bend angle and strength of lateral dipole were synthesized, and their phase behavior was characterized by polarizing microscopy, thermal analysis, X-ray diffraction, and electrooptical measurements. We find the general destabilization of the liquid crystallinity caused by strong lateral dipolar groups and the bent molecular shape are off-set in mesomorphic tetracatenars, which display stable nematic, smectic, columnar, and cubic mesophases. The broad mesomorphism of the tetracatenars containing lateral dipoles and their incompatibility with chiral induction are explained by considering that loosely correlated dimers exist within the mesophases. Chiral mesophases of derivatives with strong lateral dipoles were achieved by attaching fewer or different side chains to each end of the mesogen.

Introduction

Dipole−dipole interactions and shape anisotropy have been recognized as fundamental elements in the design of liquid crystals since the first systematic synthetic studies in the early decades of the 20th century.[1,2] More recently, microphase segregation[3] and noncovalent interactions such as H-bonding[4−6] have been added to the list of design concepts. By applying these principles, it is possible to incorporate almost any chemical structure into a liquid crystal as has been shown most notably for C_{60}.[7]

One of the present goals of synthetic liquid crystal research is to understand the interplay between different elements of design.[8] For example, molecules with unfavorable shape can be made mesogenic if favorable dipole−dipole interactions and/or microphase segregation are used to compensate for the deficiencies in shape. Exciting and surprising examples include liquid crystalline dendrimers,[9] columnar liquid crystals that lack side chains,[10] and unusually shaped amphiphilic molecules.[11]

New types of liquid crystalline phases displayed by certain bent-rod molecules (banana phases) have received much attention in recent years.[12−16] Novel ferroelectric[17,18] and antiferroelectric[19−24] mesophases were obtained from initially achiral molecules and macrophase separation of racemic mixtures[16] into homo-chiral domains was observed. However, the design principles appear to be subtle, as the majority of bent-rod (banana) mesogens did not display these new mesophases, if any mesophase at all, despite possessing similar molecular structures.[25−27] The ultimate goal of being able to accurately predict the liquid crystalline properties of many molecular structures remains elusive, despite the numerous mesomorphic

* Address correspondence to this author. e-mail: tswager@mit.edu.

(1) Demus, D.; Goodby, J.; Gray, G. W.; Spiess, H.-W.; Vill, V. In *Handbook of Liquid Crystals*; Wiley- VCH: Weinheim, 1998; Vol. 1.
(2) Kelker, H.; Hatz, R. In *Handbook of Liquid Crystals*; Wiley-VCH: Weinheim, 1980.
(3) Pegenau, A.; Hegmann, T.; Tschierske, C.; Diele, S. *Chem. Eur. J.* **1999**, *5*, 1643−1660.
(4) Kato, T. In *Handbook of Liquid Crystals*; Vill, V., Ed.; Wiley-VCH: Weinheim, 1998; Vol. 2B, pp 969−979.
(5) Nishikawa, E.; Samulski, E. T. *Liq. Cryst.* **2000**, *27*, 1463−1471.
(6) Nishikawa, E.; Samulski, E. T. *Liq. Cryst.* **2000**, *27*, 1457−1462.
(7) Dardel, B.; Guillon, D.; Heinrich, B.; Deschenaux, R. *J. Mater. Chem.* **2001**, *11*, 2814−2831.
(8) Goodby, J. W.; Bruce, D. W.; Hird, M.; Imrie, C.; Neal, M. *J. Mater. Chem.* **2001**, *11*, 2631−2636.
(9) Richardson, R. M.; Ponomarenko, S. A.; Boiko, N. I.; Shibaev, V. P. *Liq. Cryst.* **1999**, *26*, 101−108.
(10) Barbera, J.; Rakitin, O. A.; Ros, M. B.; Torroba, T. *Angew. Chem., Int. Ed. Engl.* **1998**, *37*, 296−299.
(11) Kolbel, M.; Beyersdorff, T.; Sletvold, I.; Tschierske, C.; Kain, J.; Diele, S. *Angew. Chem., Int. Ed.* **1999**, *38*, 1077−1080.
(12) Niori, T.; Sekine, T.; Watanabe, J.; Furukawa, T.; Takezoe, H. *J. Mater. Chem.* **1996**, *6*, 1231−1233.
(13) Sekine, T.; Niori, T.; Sone, M.; Watanabe, J.; Choi, S. W.; Takanishi, Y.; Takezoe, H. *Jpn. J. Appl. Phys., Part 1* **1997**, *36*, 6455−6463.
(14) Heppke, G.; Moro, D. *Science* **1998**, *279*, 1872−1873.
(15) Watanabe, J.; Niori, T.; Sekine, T.; Takezoe, H. *Jpn. J. Appl. Phys., Part 2* **1998**, *37*, L139-L142.
(16) Link, D. R.; Natale, G.; Shao, R.; Maclennan, J. E.; Clark, N. A.; Koerblova, E.; Walba, D. M. *Science* **1997**, *278*, 1924−1927.
(17) Sekine, T.; Takanishi, Y.; Niori, T.; Watanabe, J.; Takezoe, H. *Jpn. J. Appl. Phys., Part 2* **1997**, *36*, L1201-L1203.
(18) Walba, D. M.; Korblova, E.; Shao, R.; Maclennan, J. E.; Link, D. R.; Glaser, M. A.; Clark, N. A. *Science* **2000**, *288*, 2181−2184.
(19) Wang, K.; Jakli, A.; Li, H. F.; Yang, Y. G.; Wen, J. X. *Liq. Cryst.* **2001**, *28*, 1705−1708.
(20) Reddy, R. A.; Sadashiva, B. K.; Dhara, S. *Chem. Commun.* **2001**, 1972−1973.
(21) Walba, D. M.; Korblova, E.; Shao, R. F.; Maclennan, J. E.; Link, D. R.; Glaser, M. A.; Clark, N. A. *J. Phys. Org. Chem.* **2000**, *13*, 830−836.
(22) Shen, D.; Pegenau, A.; Diele, S.; Wirth, I.; Tschierske, C. *J. Am. Chem. Soc.* **2000**, *122*, 1593−1601.
(23) Wrobel, S.; Haase, W.; Kilian, D.; Chien, L. C.; Chong-Kwang, L. *Ferroelectrics* **2000**, *243*, 277−289.
(24) Heppke, G.; Parghi, D. D.; Sawade, H. *Ferroelectrics* **2000**, *243*, 269−276.
(25) Pelzl, G.; Diele, S.; Weissflog, W. *Adv. Mater.* **1999**, *11*, 707−724.
(26) Shen, D.; Diele, S.; Pelzl, G.; Wirth, I.; Tschierske, C. *J. Mater. Chem.* **1999**, *9*, 661−672.
(27) Matraszek, J.; Mieczkowski, J.; Szydlowska, J.; Gorecka, E. *Liq. Cryst.* **2000**, *27*, 429−436.

10.1021/ja0268027 CCC: $22.00

Scheme 1. Synthesis of Thiophene Based Tetracatenars[a]

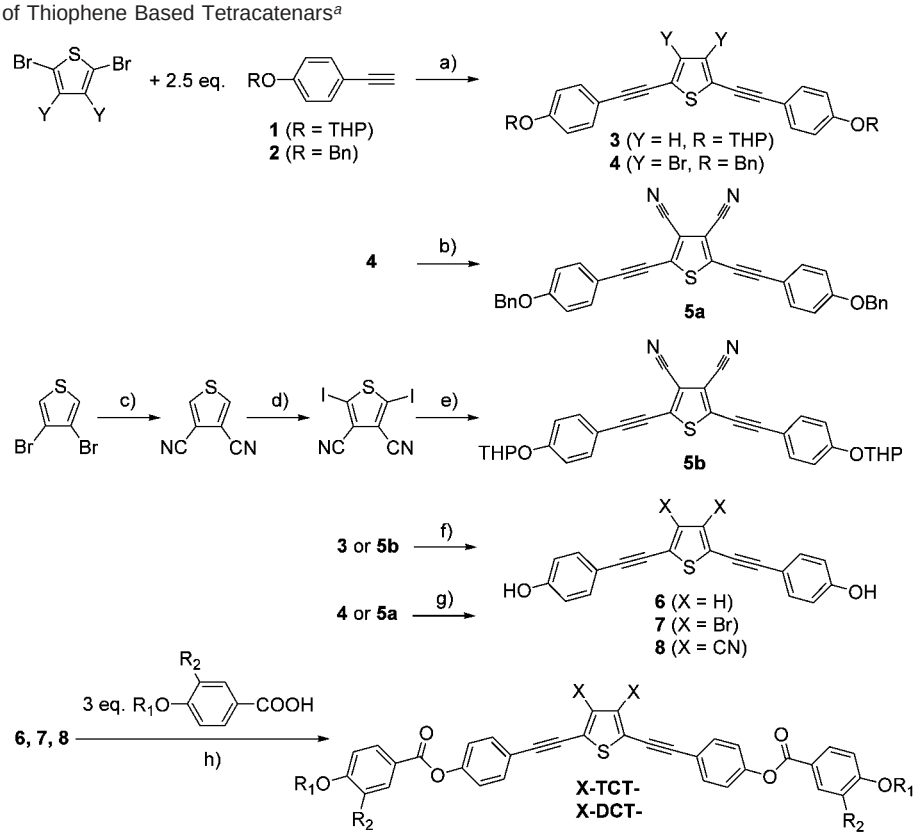

H-TCT-mp4-14: X = H; $R_1 = (C_nH_{2n+1})$, n = 4, 6, 8, 10, 12, 14; $R_2 = (OC_nH_{2n+1})$, n = 4, 6, 8, 10, 12, 14
H-TCT-mp10*(S): X = Br; $R_1 = ((S)C_2H_4C^*H(Me)C_3H_6CH(Me)_2)$; $R_2 = ((s)OC_2H_4C^*H(Me)C_3H_6CH(Me)_2)$
Br-TCT-mp4-12: X = Br; $R_1 = (C_nH_{2n+1})$, n = 4, 6, 8, 10, 12; $R_2 = (OC_nH_{2n+1})$, n = 4, 6, 8, 10, 12
Br-TCT-mp10*(S): X = Br; $R_1 = ((S)C_2H_4C^*H(Me)C_3H_6CH(Me)_2)$; $R_2 = ((s)OC_2H_4C^*H(Me)C_3H_6CH(Me)_2)$
NC-TCT-mp4-12: X = CN; $R_1 = (C_nH_{2n+1})$, n = 4, 5, 6, 7, 8, 9, 10, 11, 12;
$R_2 = (OC_nH_{2n+1})$, n = 4, 5, 6, 7, 8, 9, 10, 11, 12
NC-TCT-mp4*(S): X = CN; $R_1 = ((S)\ CH_2C^*H(Me)C_2H_6)$; $R_2 = ((S)\ OCH_2C^*H(Me)C_2H_6)$
NC-TCT-mp10*(rac);(R);(S): X = CN; $R_1 = ((S)$ or $(R)C_2H_4C^*H(Me)C_3H_6CH(Me)_2)$;
$R_2 = ((S)$ or $(R)OC_2H_4C^*H(Me)C_3H_6CH(Me)_2)$
NC-DCT-p10; 12: X = CN; $R_1 = (C_nH_{2n+1})$, n = 10, 12; R_2 = H
NC-DCT-p4*(S): X = CN; $R_1 = ((S)CH_2C^*H(Me)C_2H_5)$; R_2 = H
NC-DCT-p10*(S): X = CN; $R_1 = ((S)C_2H_4C^*H(Me)C_3H_6CH(Me)_2)$; R_2 = H

[a] (a) Pd $(PPh_3)_4$, CuI, iPr_2NH, toluene, 25 °C, >90%. (b) and (c) CuCN, CuI, DMI, 120 °C, 3.5 h, >60%. (d) 2.2 equiv LDA, I_2, THF, −78 °C, 77%. (e) Pd $(PPh_3)_4$, CuI, iPr_2NH, toluene, 25 °C, >90%. (f) TsOH, MeOH, 25 °C, >90%. (g) BrB-catechol, DCM, 0−25 °C, >90%. (h) (iPr)N═C═N(iPr), DMAP, DCM, 0−25 °C, 70−90%.

molecular structures and liquid crystalline phases that have been studied over the last hundred years.

We have been investigating thiophene-based, bent-rod mesogens which contain lateral dipolar groups attached to the thiophene in the center of the molecule.[28,29] In a preliminary study on the mesomorphism of bent-rod 2,5-bis(4-alkoxyphenylacetylene)thiophene derivatives,[29] we found that molecules with local lateral dipoles of up to 6.3 D at the central thiophene ring displayed nematic mesophases, and single-crystal structures revealed a dimer formation of neighboring molecules with an antiparallel orientation of their dipoles. Antiparallel packing was also found in the hexagonal columnar mesophase of the hexacatenar (six side chains) 2,5-bis[4-(3,4,5-tridodecyloxyphenylcarbonyloxy)phenylethynyl]-3,4-dicyanothiophene.[28]

We now present an expanded study on the effects of bend angle, lateral dipole, chirality, and symmetry on the liquid crystalline properties of thiophene-based polycatenar liquid crystals. The tetracatenar (four side chains) and tricatenar (three side chains) structures allow us to access a wide variety of mesophases simply by changing the length, number, and position of side chains. Nematic (N), smectic (Sm), columnar (Col), and cubic mesophases of polycatenars were obtained as well as chiral-nematic (N*) and smectic C (SmC*) phases. Their potential as new building blocks for polar materials is discussed.

Results and Discussion

Synthesis. To guide the reader through the many structures reported herein, we have developed the following nomenclature system. The mesogenic cores are described as catenars with DC standing for dicatenar, TrC standing for tricatenar, and TC standing for tetracatenar. The very central portion of the core is either a 2,5-thienyl (XXT), para-phenyl (pXXP), or meta-phenyl (mXXP) where the XX represents the type of catenar. The central rings of the core can be substituted with hydrogens (H), bromides (Br) or nitriles (NC) as shown in Schemes 1 and 2. Hence, NC-TCT stands for a nitrile containing tetracatenar

(28) Levitsky, I. A.; Kishikawa, K.; Eichhorn, S. H.; Swager, T. M. *J. Am. Chem. Soc.* **2000**, *122*, 2474−2479.
(29) Kishikawa, K.; Harris, M. C.; Swager, T. M. *Chem. Mater.* **1999**, *11*, 867−871.

Scheme 2. Synthesis of Unsymmetric and Benzene Based Polycatenars[a]

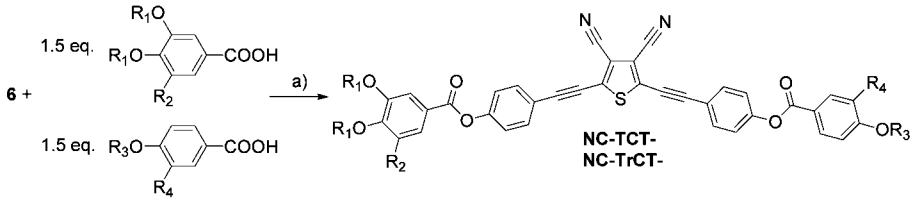

NC-TCT-mp6,mp10*(R): $R_1 = (C_6H_{13})$, $R_2 = H$, $R_3 = ((S)\ C_2H_4C^*H(Me)C_3H_6CH(Me)_2)$, $R_4 = OR_3$
side products are **NC-TCT-mp6** and **NC-TCT-p10*(R)**

NC-TrCT-mp4,p10*(S): $R_1 = (C_4H_9)$, $R_2 = H$, $R_3 = ((S)\ C_2H_4C^*H(Me)C_3H_6CH(Me)_2)$, $R_4 = H$
side products are **NC-TCT-mp4** and **NC-DCT-p10*(S)**

NC-TrCT-mp6,p10*(S): $R_1 = (C_6H_{13})$, $R_2 = H$, $R_3 = ((S)\ C_2H_4C^*H(Me)C_3H_6CH(Me)_2)$, $R_4 = H$
side products are **NC-TCT-mp6** and **NC-DCT-p10*(S)**

NC-TCT-mpm12,p8: $R_1 = (C_{12}H_{25})$, $R_2 = OR_1$, $R_3 = (C_8H_{17})$, $R_4 = H$
side products are the hexacatenar and the dicatenar

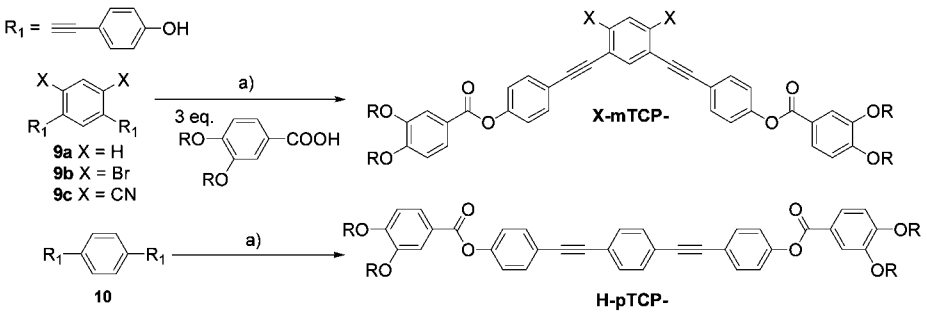

H-mTCP-mp6; 10: X = H; $R = (C_nH_{2n+1})$, n = 6, 10
Br-mTCP-mp6; 8; 10; 12: X = Br; $R = (C_nH_{2n+1})$, n = 6, 8, 10, 12
NC-mTCP-mp8; 12: X= CN; $R = (C_nH_{2n+1})$, n = 8, 12
H-pTCP-mp6; 10: $R = (C_nH_{2n+1})$, n = 6, 10

[a] (a) (iPr)N═C═N(iPr), DMAP, DCM, 0-25 °C, 70-85%.

Table 1. Mesomorphism of the Symmetric Thiophene and 3,4-Dibromothiophene- Based Tetracatenars Determined by Polarizing Microscopy, DSC (5 °C/min) and X-ray Diffraction

compound	transition	*T*/deg C, heating (ΔH/kJ mol^{-1})	*T*/deg C, cooling (ΔH/kJ mol^{-1})	compound	transition	*T*/deg C, heating (ΔH/kJ mol^{-1})	*T*/deg C, cooling (ΔH/kJ mol^{-1})
H−TCT−mp4				**Br-−TCT−mp4**	Cr−(N)[a]	135.2 (57.03)	87.1 (−28.31)
					(N)−I		133.9 (−1.10)
H−TCT−mp6	Cr−N	137.6 (69.88)	122.9 (−67.77)	**Br−TCT−mp6**	Cr−(N)[a]	189.6 (95.28)	127.9 (−55.14)
	N−I	144.1 (1.11)	142.9 (−1.14)		(N)−I		161.1 (−1.22)
H−TCT−mp8	Cr−(N)[a]	138.1 (74.57)	117.6 (−73.14)	**Br−TCT−mp8**	Cr−(N)[a]	119.5 (52.93)	84.8 (−51.14)
	(N)−I		133.2 (−1.22)		(N)−I		107.6(−1.01)
H−TCT−mp10	Cr−(SmC)[a]	127.3 (71.58)	112.0 (−62.11)	**Br−TCT−mp10**	Cr−(SmC)[a]	110.8 (47.86)	82.7 (−98.56)
	(SmC)−(N)		114.8 (−6.92)		(SmC)−I		97.3 (−7.51)
	(N)-I		125.9 (−1.09)				
H−TCT−mp12	Cr−(N)[a]	133.6 (89.77)	116.9 (−87.66)	**Br−TCT−mp12**	Cr−(SmC)[a]	117.3 (67.74)	89.4 (−53.95)
	(N)-I		120.5 (−1.26)		(SmC)−I		98.3 (−3.16)
H−TCT−mp14	Cr−I	125.4 (91.41)	115.3 (−98.49)	**Br−TCT−mp10*(S)**	Cr−I	103.3 (42.74)	60.9 (−47.01)
H-−TCT−mp10*(S)	Cr−I	99.2 (66.39)	63.2 (−44.49)				

[a] Monotropic mesophases in brackets.

based on the 2,5-thienyl group. At the ends of the mesogens are benzoates containing alkyl-oxy side chains that are para (p) or meta (m) with respect to the ester, and for example, a mpm12 designation indicates that 12 carbon alkyl-oxy side chains are attached to both of the meta positions in addition to the para position of the benzoate. Chiral compounds are labeled (*), and the stereochemistry is given as R, S, or rac. The connectivity of the chiral side chains is shown in Schemes 1 and 2.

We chose a 2,5-bis(4-hydroxyphenylacetylene)thiophene **6** and its derivatives **7** and **8**, all fluorescent compounds, as central building blocks (Scheme 1). They were obtained in three steps from 2,5-dibromothiophene or tetrabromothiophene in analogy to previously published procedures.[28,29] Palladium-catalyzed cross-coupling of 4-(benzyloxy)phenylacetylene **2** with tetrabromothiophene results in selective substitution of the bromine atoms in the 2 and 5 positions to give **4**, which was subsequently treated with CuCN/CuI in 2,5-dimethylimidazlidinone at 120 °C to give the 3,4-dicyanothiophene derivative **5a**. Monitoring the cyanation by thin-layer chromatography suggests rapid substitution of the first bromide, while the substitution of the second bromide was much slower and was accompanied by several side reactions. Polymerization and exchange of the second bromine by hydrogen were the most prominent side reactions, and were responsible for the only moderate yields of

Table 2. Mesomorphism of the Symmetric 3,4-Dicyanothiophene-Based Tetracatenars Determined by Polarizing Microscopy, DSC (5 °C/min) and X-ray Diffraction (2D-waxs)

compound	transition	*T*/deg C, heating (ΔH/kJ mol^{-1})	*T*/deg C, cooling (ΔH/kJ mol^{-1})	*d*-values/Å (sample temp degC)[a]	tilt angle/deg SmC phase[b]
NC−TCT−mp4	Cr−N	148.4 (44.40)[c]	129.2 (−44.04)		
	N−I	162.5 (1.14)	161.4 (−1.03)		
NC−TCT−mp5	Cr−N	133.5 (40.33)[c]	116.8 (−40.87)	29.3, 3.9 (145)	
	N−I	147.6 (0.94)	146.4 (−1.67)		
NC−TCT−mp6	Cr−SmC	113.9 (32.37)	98.9 (−21.83)	28.9, 14.6, 6.3, 4.5	38
	SmC−N	121.6 (7.08)	121.6 (−7.42)	(118);	
	N−I	144.4 (0.96)	142.8 (−0.96)	30.4, 4.0 (134)	
NC−TCT−mp7	Cr−SmC	127.1 (46.46)	91.8 (−19.85)	31.5, 15.5, 6.3, 4.6	53
	SmC−I	129 (shoulder)	125.2 (−5.02)	(120)	
NC−TCT−mp8	Cr−SmC	131.2 (39.89)	109.9 (−38.48)	30.9, 15.5, 6.4, 4.7	54
	SmC−I	135.3 (6.92)	132.4 (−7.72)	(133)	
NC−TCT−mp9	Cr−SmC	119.3 (35.27)	98.9 (−30.22)	32.6, 16.4, 6.5, 4.7	56
	SmC−I	130.9 (5.50)	129.4 (−5.92)	(130)	
NC−TCT−mp10	Cr−SmC	100.5 (50.88)	86.8 (−49.88)	34.5, 17.6, 6.8, 4.7	
	SmC−Col_h	123.4 (2.95)	111.7 (−4.38)	(110);	
	Col_h-I	131.4 (3.95)	129.7 (−3.66)	39.0, 22.5, 19.7, 6.5, 4.6 (130)	
NC−TCT−mp11	Cr−Col_h	106.2 (59.99)[d]	94.7 (−61.61)	39.9, 23.2, 20.2, 6.8,	
	Col_h−I	137.5 (5.29)	136.1 (−4.19)	4.7 (120)	
NC−TCT−mp12	Cr−Col_h	102.8 (89.29)	87.8 (−81.35)	41.1, 23.9, 20.8,	
	Col_h−I	138.0 (2.78)	130.3 (−6.79)	6.3(small),4.7 (115)	
NC−TCT−mp4*(S)	Cr−I	161.0 (31.38)	107.2 (−34.33)		
NC−TCT−mp10*(rac)	Cr−(N)	101.6 (62.89)	69.4 (−37.88)		
	(N)−I		74.7 (−2.14)		
NC−TCT−mp10*(R),(S)	Cr−I	104.1 (56.57)	66.9 (−15.62)[e]		

[a] Reflections at 6−7 Å and 4−5 Å are broad halos. [b] Angle between layer and side-chain reflections of magnetically aligned samples. [c] Nematic phases were not observed at the first heating runs since the Cr−I transitions were at 189.0 (79.63) for **mp−TC−4** and at 154.8 (56.67) for **mp−TC−5**. [d] A Cr−SmC transition was observed on the first heating run, 110.6 (2.94) [e] Cold crystallization on heating run.

about 60%. Cleavage of the benzyl-protecting groups in **4** and **5a** with *B*-bromocatecholborane afforded the diphenolic building blocks **7** and **8**, respectively, in good yields. The same synthetic approach was initially applied to obtain **6**, but the cleavage of the benzyl groups with boroncatecholbromide or BBr_3 was low-yielding due to the occurrence of side-reactions. Compound **6** was therefore synthesized via the tetrahydropyran (THP)-protected precursor **3**.

An alternative synthetic approach to **8** involves cyanation of 3,4-dibromothiophene followed by the lithiation and subsequent iodination of the 2 and 5 positions (Scheme 1). The resulting 2,5-diiodo-3,4-dibromothiophene was then converted to **5b** via palladium-catalyzed cross-coupling. The 42% overall yield of this pathway is similar to the yield obtained for the approach described above, but the lowest-yielding cyanation step is carried out at the beginning of the synthetic scheme, with the result that purification of the following intermediates is much easier.

Esterification of the lateral hydroxy groups of **6**−**8** with the corresponding benzoic acid derivatives in the presence of diisopropylcarbodiimide and 4-(dimethylamino)pyridine gave the desired symmetric di- and tetracatenars (Scheme 1) in good yields. Polycatenars possessing two different benzoic ester groups were obtained by statistical mono-esterification and subsequent chromatographic separation of the two symmetric side products (Scheme 2). 1,3-Bis(4-hydroxyphenylacetylene)-benzene (**9a**) and 1,4-bis(4-hydroxyphenylacetylene)benzene (**10**) derivatives were synthesized for comparison purposes (Scheme 2). The reaction pathways were identical to the preparation of **6** and **H-TCT-mp4-14** except that 1,3-dibromobenzene and 1,2-dibromobenzene were used as central cores instead of 2,5-dibromothiophene. Experimental details are given as Supporting Information.

Mesomorphism. The phase diagrams of all compounds were determined by temperature controlled polarizing microscopy, differential scanning calorimetry (DSC), and X-ray diffraction. All diffraction data agreed with our phase assignments, and details are given for higher ordered enantiotropic mesophases. The results for the thiophene based symmetric tetracatenars are summarized in Tables 1 and 2. Tables 3 and 4 contain the data for the symmetric dicatenars, the unsymmetric tri and tetracatenars, as well as the bistolane-based straight-rod tetracatenars.

Incorporation of a bent core within a molecular design typically destabilizes the resulting liquid crystalline phases as the bent-rod shape of the molecules interferes with their rotational freedom.[30−33] Both the **H-TCT-mp** as well as **Br-TCT-mp** tetracatenar derivatives follow this trend (Table 1). Despite possessing moderate bend angles (154°) these compounds display exclusively monotropic mesophases (with the exception of the nematic phase of **H-TCT-mp6**). This stands in direct contrast to the corresponding straight-rod tetracatenars **H-CPpTCP-mp6** and **-mp10**, which exhibit SmC and N phases over wide temperature ranges, suggesting that the introduction of even small bend angles has dramatic consequences upon the stability of the resulting liquid crystal phases of these compounds (Table 4). As one would expect, further increasing the bend to 120° as in the **H-mTCP-mp** and **Br-mTCP-mp** derivatives exaggerates the effect and in fact results in the complete suppression of mesomorphism (Table 4).

(30) Friedman, M. R.; Toyne, K. J.; Goodby, J. W.; Hird, M. *J. Mater. Chem.* **2001**, *11*, 2759−2772.
(31) Fazio, D.; Mongin, C.; Donnio, B.; Galerne, Y.; Guillon, D.; Bruce, D. W. *J. Mater. Chem.* **2001**, *11*, 2852−2863.
(32) Dingemans, T. J.; Samulski, E. T. *Liq. Cryst.* **2000**, *27*, 131−136.
(33) Dingemans, T. J.; Murthy, N. S.; Samulski, E. T. *J. Phys. Chem. B* **2001**, *105*, 8845−8860.

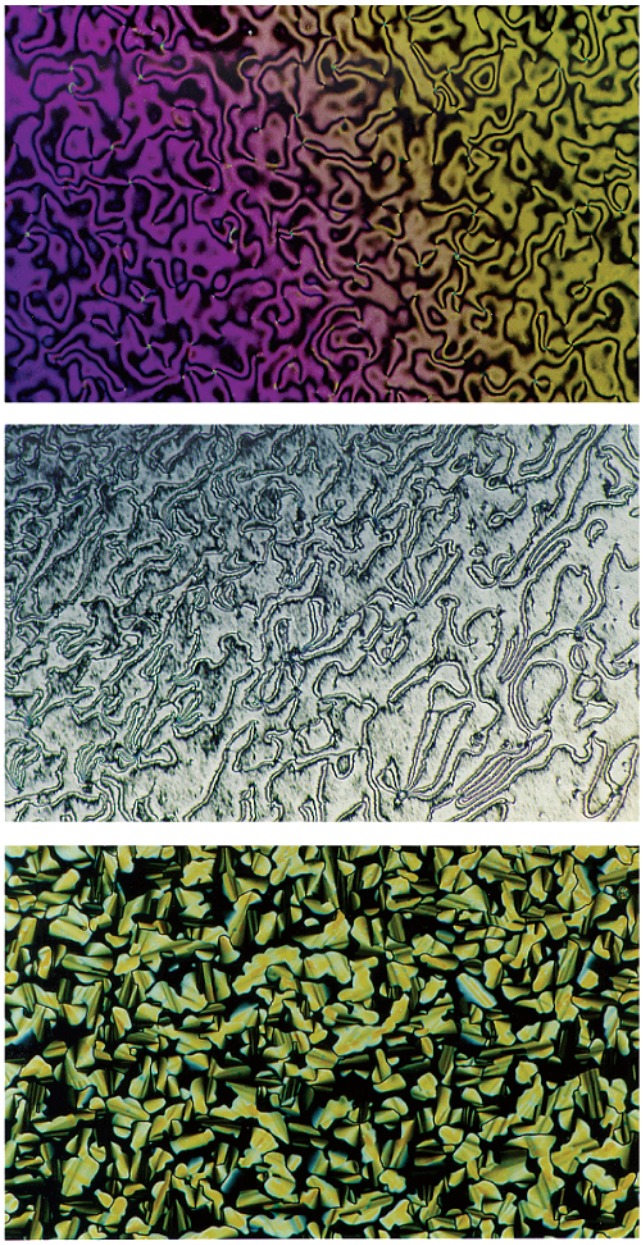

Figure 1. Microphotographs of the nematic Schlieren texture of **mp-TC-4** at 162 °C (×160) [top], the SmC Schlieren texture of **mp-TC-8** at 115 °C (×200) [middle], and the pseudofocal conic type texture of the Col_h mesophase of **mp-TC-10** at 124 °C (×320) [bottom]. All samples were sandwiched between untreated glass slides and viewed through crossed polarizers

We found that the introduction of a strong lateral dipole through the incorporation of cyano groups at the 3 and 4 positions of the central thiophene unit changes the mesomorphic properties of the tetracatenars. The **NC-TCT-mp** derivatives are liquid crystalline over wide temperature ranges and display a polymesomorphism typical of tetracatenars (Table 2). The types of mesophases progress from N, to SmC, to Col with increasing side chain length (Figure 1). X-ray tilt angle measurements on magnetically aligned samples reveal a constant increase of tilt angle of the SmC phases from **NC-TCT-mp6** to **NC-TCT-mp9** with the SmC phase of **NC-TCT-mp10** eventually converting into a high-temperature hexagonal columnar mesophase (Col_{hex}). This behavior is typical of tetracatenars and is consistent with a model in which the increasing steric demand of the side chains causes the phase transition from SmC to Col.[34,35] A cubic mesophase is displayed by **NC-TCT-mpm12,p8** which is also a reported behavior of classical tetracatenars with three terminal side chains at one end and only one side chain at the other end.[36]

The strong lateral dipole (calculated to be 6.3 D) and steric hindrance introduced by the two cyano groups increases the rotational barrier about the long axis of the mesogens and results in strong intermolecular dipole−dipole interactions. Both of these effects would be expected to promote higher melting points and decreased mesomorphism. Following this line of reasoning, tetracatenars **H-TCT-mp** (with the smallest lateral dipoles and least steric hindrance to rotation) would have been predicted to display mesophases that were significantly more stable than those of the **NC-TCT-mp** analogues, which is in direct contrast to our observations.

We believe that the unexpectedly broad mesomorphism of the **NC-TCT-mp** derivatives can be reasoned by considering two factors. First, the individual **NC-TCT-mp** molecules form loosely associated dimers with antiparallel dipole orientations that function as the mesomorphic unit in the liquid crystalline phase. While strict antiparallel association of nearest-neighbor molecules has not been observed for calamitic liquid crystals, several classical nematic and smectic liquid crystals with strong dipoles along their molecular long axis, such as cyanobiphenyl type systems,[37] have been shown to statistically adopt antiparallel orientations. The formation of these dimers results in a mesomorphic unit in which the deleterious effects of both the bent-shape and large lateral dipoles are largely negated, as such a dimer sweeps out an approximately cylindrical volume upon rotation around its long axis. Experimental support of our hypothesis was provided by antiparallel dimer formation in single crystals of related compounds[29] and by two-dimensional X-ray diffraction data of magnetically aligned Col_{hex} and SmC mesophases. A weak and diffuse peak centered at 0.75 nm, the expected distance between the sulfur atoms of every other thiophene unit in stacks of alternating antiparallel packing, was found in all of the diffraction patterns (Figure 2). A similar but sharper peak was found in the X-ray diffraction pattern of a related hexacatenar derivative, for which antiparallel columnar packing was independently verified by photophysical methods.[28] Second, the lateral dipole introduced by the two cyano groups is likely to influence the conformation of the tetracatenars driven by the intramolecular interactions between the dipoles of the cyano groups, the ester groups, and the alkoxyphenyl ether groups. Semiempirical calculations on individual molecules in the gas phase reveals four low-energy conformers (Figure 3). Their overall shape (bend) and lateral dipole vary considerably, which emphasizes the wide range of conformations these molecules are able to adapt despite their rigid bent core. The terminal benzoic ester groups can either oppose or enhance the bend of the central 2,5-bis(phenylacetylene)thiophene entity and can impart an overall more bent, more elongated, or zigzag shape to the molecules.

The two conformers found in the single-crystal structures of

(34) Nguyen, H. T.; Destrade, C.; Malthête, J. *Adv. Mater*. **1997**, *9*, 375−387.
(35) Rais, K.; Daoud, M.; Gharbia, M.; Gharbi, A.; Nguyen, H. T. *ChemPhysChem* **2001**, *2*, 45−49.
(36) Nguyen, H. T.; Destrade, C.; Malthete, J. In *Handbook of Liquid Crystals*; Demus, D.; Goodby, J.; Gray, G. W.; Spiess, H.-W.; Vill, V., Eds.; Wiley-VCH: Weinheim, 1998; Vol. 2B, pp 865−900.
(37) Cook, M. J.; Wilson, M. R. *Liq. Cryst.* **2000**, *27*, 1573−1583.

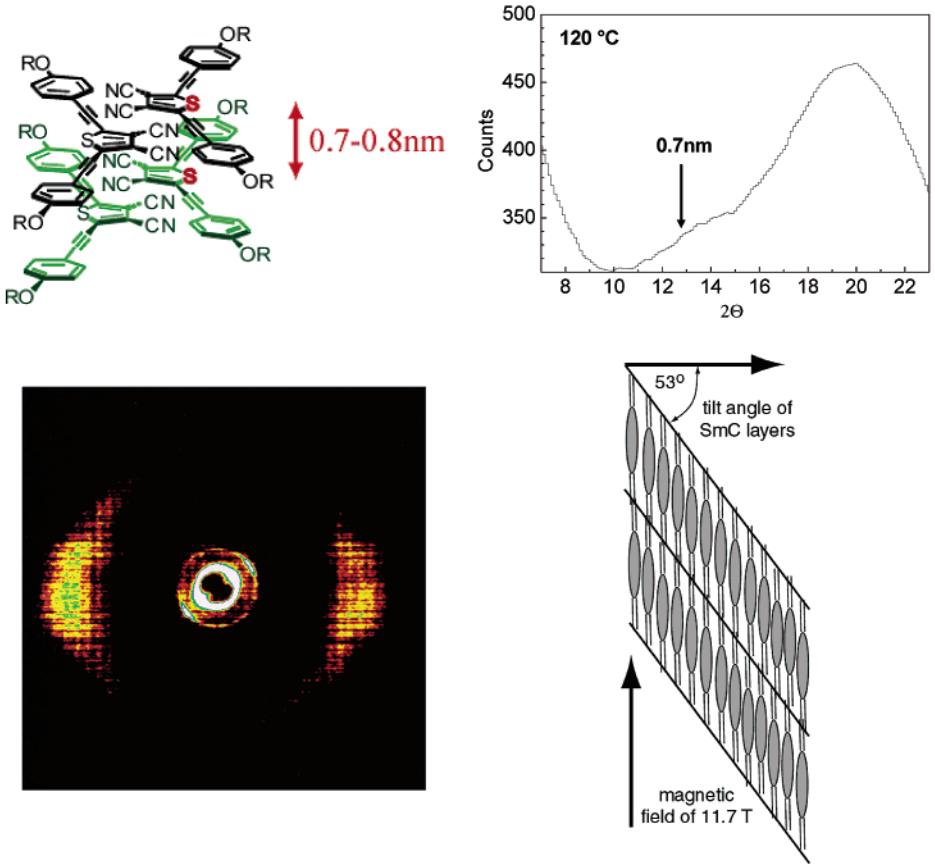

Figure 2. (a) 1D X-ray diffraction pattern (wide-angle region) of sample **mp-TCT-7** at 120 °C and illustrated antiparallel packing of molecules. (b) 2D X-ray diffraction pattern of a previously magnetically aligned sample of **mp-TCT-7** at 120 °C, which shows a 53° tilt angle in the SmC phase.

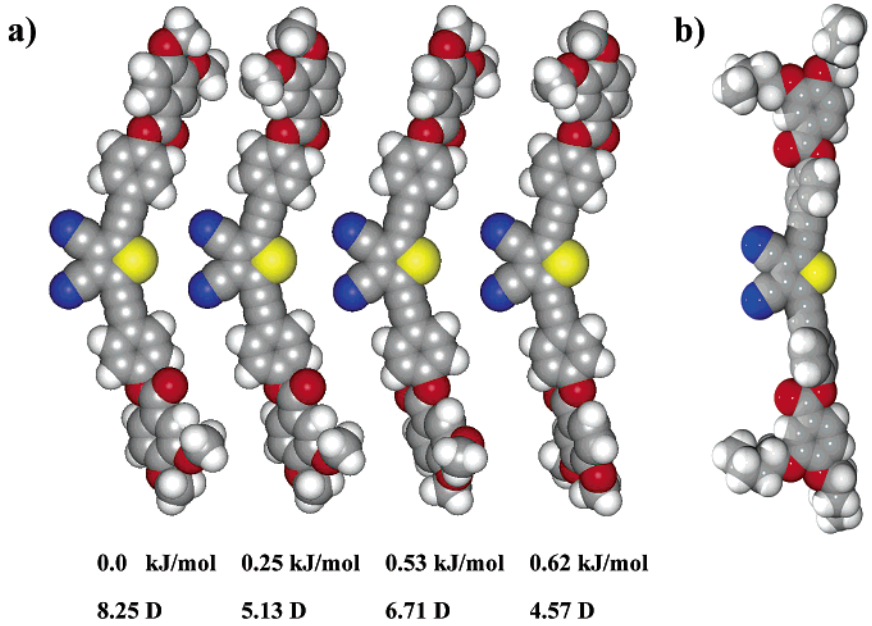

Figure 3. (a) Four lowest-energy conformers of a **NC-TCT-mp** derivative with methoxy groups. The conformer minima were first determined by molecular mechanics (MMFF94) and subsequent energy minimization by AM1 calculations in Spartan. (b) A conformation in which the dipoles of the carbonyl groups and cyano goups point toward the same direction was found in the single-crystal structure of **NC-TCT-mp4** shown for comparison.

NC-TCT-mp4 and **NC-DCT-p4*** were very different (Figures 3 and 4); this is possibly due to molecular packing forces. **NC-TCT-mp4** showed an interdigitated structure with antiparallel dipoles, while **NC-DCT-p4*** displayed layers with parallel dipole orientation within a layer. While the large hysteresis (>10 °C) in the melting transition temperatures of the **NC-TCT-mp** compounds suggests major structural changes are occurring at the crystal−mesophase transitions and that the single-crystal structure is therefore unlikely to reflect the order in the liquid crystalline phase, the crystal structure does help to elucidate generally favored and disfavored intermolecular interactions as well as conformations. **NC-mTCP-mp** bistolane derivatives

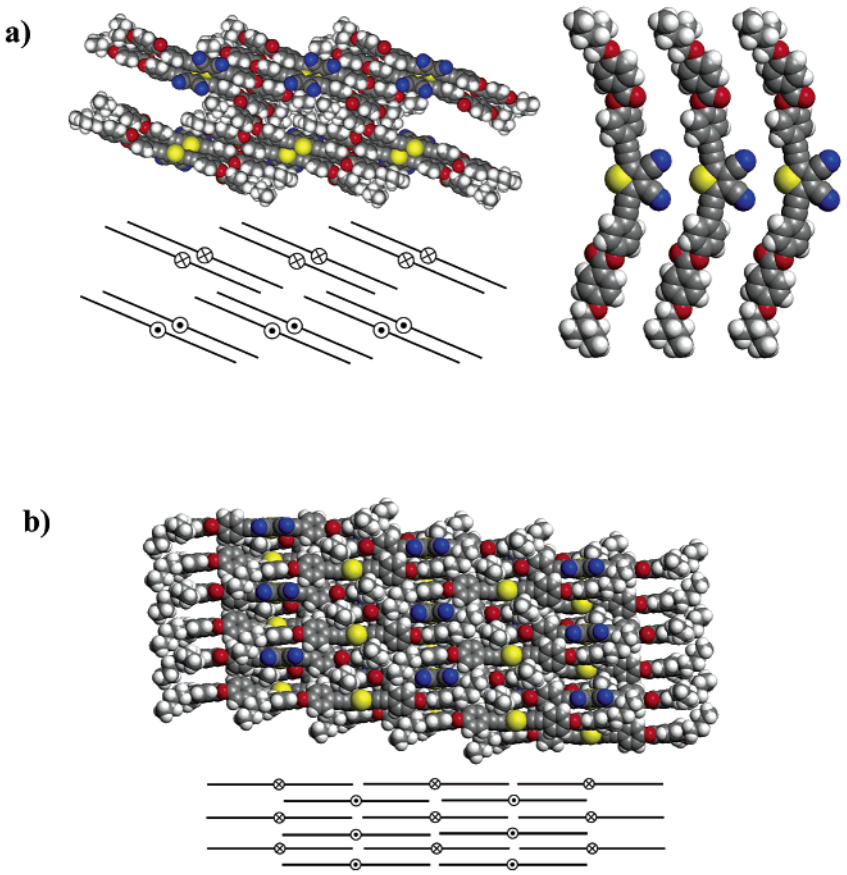

Figure 4. Molecular packing in the single-crystal structures of (a) **NC-DCT-p4*** with polar layer structure and (b) nonchiral **NC-TCT-mp4** with interdigitated antiparallel dipole orientation.

Table 3. Mesomorphism of 3,4-Dicyanothiophene-Based Symmetric Dicatenars as Well as Unsymmetric Tricatenars and Tetracatenars Determined by Polarizing Microscopy, DSC (5 °C/min) and X-ray Diffraction

compound	transition	*T*/deg C, heating (Δ*H*/kJ mol^{-1})	*T*/deg C, cooling (Δ*H*/kJ mol^{-1})	*d*-values/Å (sample temp/degC)[a]
NC−DCT−p10	Cr−SmC	143.5 (12.74)	119.4 (−10.65)	
	SmC−N	196.1 (0.64)	192.0 (−0.57)	
	N−I	281.8 (0.12)	279.9 (−0.12)	
NC−DCT−p12	Cr−N	131.4 (29.68)	111.1 (−11.40)	
	N−I	221.9 (0.48)	220.1 (−0.72)	
NC−DCT−p4*(S)	Cr−N*	206 (24.76)	198 (−22.03)	
	N*−I	279 (0.14)	278 (−0.11)	
NC−DCT−p10*(S)	Cr−SmC*	158.8 (39.95)	125.9 (−33.84)	29.6, 14.9, 4.5
	SmC*−N*	171.9 (2.002)	171.8 (−1.47)	(165 °C)
	N*−I	247.6 (0.94)	233.8 (−0.12)	
NC−TrCT−mp4,p10*(S)	Cr−(SmC*)[b]	157.2 (55.59)	122.2 (−40.85)	
	(SmC*)−N*	213.2 (1.22)	127.5 (−2.54)	
	N*−I		210.8 (−1.16)	
NC−TrCT−mp6,p10*(S)	Cr−SmC*	138.7 (39.81)	104.7 (−30.76)	30.3, 15.2, 4.5
	SmC*−N*	146.2 (4.23)	145.5 (−4.26)	(130 degC)
	N*−I	194.1 (1.09)	193.3 (−1.09)	
NC−TCT−mp6, mp10*(R)	Cr−SmC*	92.8 (32.33)	54.0 (−16.11)	30.0, 15.1, 4.5
	SmC*−I	100.7 (5.18)	98.6 (−5.44)	(80 deg C)
NC-TCT−pm12,p8	Cr−cubic	65.6 (82.61)	41.7 (−24.37)	58(shoulder), 44,
	cubic−I	115.1 (1.80)	109.5 (−0.94)	39(shoulder), 12.5, 10.5, 6.2, 5.3, 4.5, 4.2 (68 deg C)

[a] Reflections at 6−7 and 4−5 Å are broad halos. [b] Monotropic mesophase.

(with a bend angle of 120°) cannot adapt rodlike elongated conformations and are not mesomorphic, despite their surprisingly low melting and crystallization temperatures between 116 °C and 93 °C (Scheme 2 and Table 4).

The **NC-TCT-mp** derivatives were considered candidates to display biaxial nematic phases because of the sterically and electronically hindered rotation about their molecular long axis. A tendency of mesogens to display antiparallel dimeric correlations results in mesomorphic units that may not contain lateral dipoles and a more rodlike shape. Apparently, dimers can rotate freely, and no evidence for the existence of biaxiality was found by optical microscopy.[38] However, more elaborate

Table 4. Mesomorphism of Bistolane-Based Symmetric Tetracatenars Determined by Polarizing Microscopy, DSC (5 °C/min) and X-ray Diffraction (2D-WAXS)

compound	transition	*T*/deg C, heating (ΔH/kJ mol^{-1})	*T*/deg C, cooling (ΔH/kJ mol^{-1})	*d*-values/Å (sample temp/deg C)[a]
H−mTCP−mp6	Cr−I	122 (73.79)	98.0 (−68.56)	
H−mTCP−mp10	Cr1−Cr2	95.9 (71.79)	89.6 (−71.76)	
	Cr2−I	101.2 (13.60)		
Br−mTCP−mp6	Cr−I	127.9 (56.91)[b]	82.0 (−50.81)	
Br−mTCP−mp8	Cr−I	108.9 (43.22)	88.8 (−46.43)	
Br−mTCP−mp10	Cr1−Cr2	71.5 (17.52)	89.8 (−44.89)	
	Cr2−I	109.4 (36.79)		
Br−mTCP−mp12	Cr1−Cr2	83.5 (11.69)[c]	76.1 (−4.08)	
	Cr2−I	108.4 (49.16)	82.8 (71.18)	
NC−mTCP−mp8	Cr1−Cr2	66.31 (11.43)	66.2 (−7.03)	
	Cr2−I	116.5 (39.04)	95.5 (−39.03)	
NC−mTCP−mp12	Cr1−Cr2	84.2 (42.38)	83.1 (−39.31)	
	Cr2−I	110.2 (122.56)	93.7 (123.78)	
H−pTCP−mp6	Cr−SmC	147.5 (28.61)	141.0 (−33.17)	27.9, 13.8, 4.5
	SmC−N	164.9 (9.57)	167.5 (−8.31)	(155 deg C)
	N−I	217.8 (1.47)	217.7 (−1.67)	
H−pTCP−mp10	Cr−SmC	114.6 (58.15)	112.6 (−59.66)	31.6, 15.8, 4.5
	SmC−N	159.7 (5.10)	163.3 (−5.12)	(140 deg C)
	N−I	175.7 (0.67)	174.6 (−1.18)	

[a] Reflections at 6−7 and 4−5 Å are broad halos. [b] Cold crystallization on heating at 109 °C. Cold crystallization at 97 °C.

NMR measurements would be required to provide conclusive evidence of the formation of dimers and the presence or absence of biaxiality within the phases.[39]

Control over the macroscopic alignment of liquid crystals is essential to many optical investigations and applications. Homogeneous (parallel) alignment was easily achieved for all of the symmetric tetracatenars by either the use of surface treatments such as rubbed polyimide or the application of shear forces. Homeotropic (vertical) alignment in glass cells treated with cetyl trimethylammonium bromide or octadecyltrimethoxysilane was not successful for the materials reported herein, and small, slightly tilted domains were obtained. The inability to achieve vertical alignment seems to be an attribute of the tetracatenar substitution rather than of the bent-rod structure. Bent-rod dicatenars **NC-DCT-p10**, **12** showed a better homeotropic alignment under the same conditions, while the straight-rod tetracatenars **H-pTCP-mp6**, **10** did not. We considered that the high clearing temperatures of some of the derivatives could be problematic, but reference measurement with known liquid crystals did not suggest any thermal damage to the alignment layers when heated to temperatures up to 220 °C.

Untreated hydrophilic surfaces resulted in a preferred homogeneous organization of **NC-TCT** derivatives that can be explained due to surface interactions with the lateral polar cyano groups. All **NC-TCT** derivatives were further investigated as free-standing films, and the fact that **NC-TCT-mp4**, **-5**, and **-6** display stable freely suspended films is noteworthy, because few nematic liquid crystals are capable of this behavior.[38,40] These compounds show easily interpretable defect textures as free-standing films, whereas on solid surfaces unusual and small domain defect textures are often observed due to the strong surface interactions of their bent-rod shapes and large lateral dipoles. Figure 5 shows a sequence of textures monitoring the Col_h to SmC transition of **NC-TCT-mp10** in a free-standing film of 1 mm diameter. In these photographs, the texture changes from fanlike to Schlieren-like, which indicates a transition from a homogeneously aligned columnar to a homeotropically aligned smectic phase.

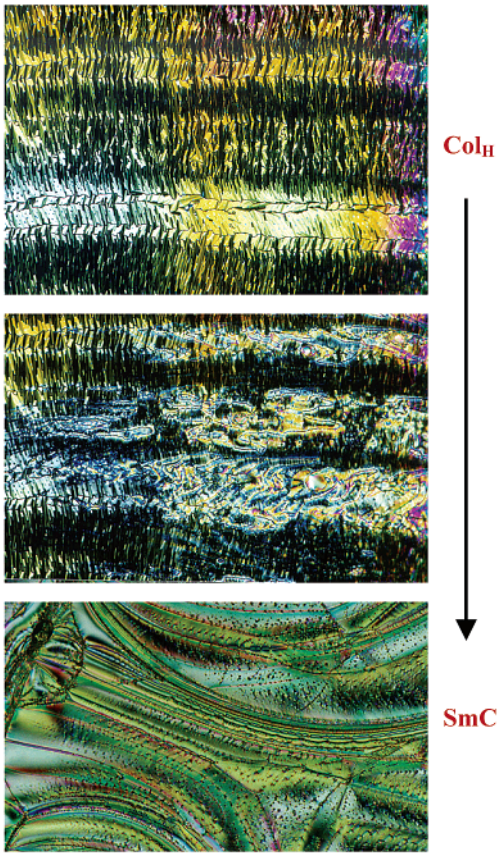

Figure 5. Phase transition from a Col_h to a SmC phase in a free-standing film of **NC-TCT-mp8** (on cooling, ×200).

As none of the aforementioned liquid crystals display ferroelectric or antiferroelectric mesophases, we decided to introduce chiral side chains to induce polar phases in **NC-TCT-mp** derivatives. This effort was encouraged by the polar sheet structure found in the single-crystal structure of **NC-DCTp4*-(S)**. A parallel orientation of the cyano-groups of neighboring molecules within each sheet was revealed, but the overall material was not polar since the orientation of the macroscopic dipole alternates from sheet to sheet (Figure 4).

Surprisingly, the introduction of four chiral branched side chains fully suppressed liquid crystallinity of the derivatives **X-TCT-mp10*** and **NC-TCT-mp4***. Only the 8-stereoisomer mixture **NC-TCT-mp10*(rac)**, derived from the attachment of racemic side chains, displayed a monotropic N-phase. Similarly, a narrow enantiotropic nematic mesophase (4 °C) was exhibited by the 1:1 mixture of the (R) and (S) enantiomers.

An explanation for the suppression of the liquid crystallinity in systems with chiral side chains is that disturbances caused by the methyl-group branches of the chiral side chains push the molecules apart. Models show that this steric hindrance is even stronger when we assume that antiparallel packing is preferred, since this organization results in the methyl groups being directed toward each other rather than all pointing in a similar direction such as is the case in a SmC*. A 1:1 mixture of the (R) and (S) enantiomers results in a decreased disturbance, and consistent with this model, the 1:1 mixture was the only

(38) Chandrasekhar, S.; Nair, G. G.; Shankar Rao, D. S.; Krishna Prasad, S.; Praefcke, K.; Blunk, D. *Liq. Cryst.* **1998**, *24*, 67−70.
(39) Hunt, J. J.; Date, R. W.; Timimi, B. A.; Luckhurst, G. R.; Bruce, D. W. *J. Am. Chem. Soc.* **2001**, *123*, 10115−10116.
(40) Faetti, S.; Palleschi, V. *Phys. Rev. A: At., Mol., Opt. Phys.* **1984**, *30*, 3241−3251.

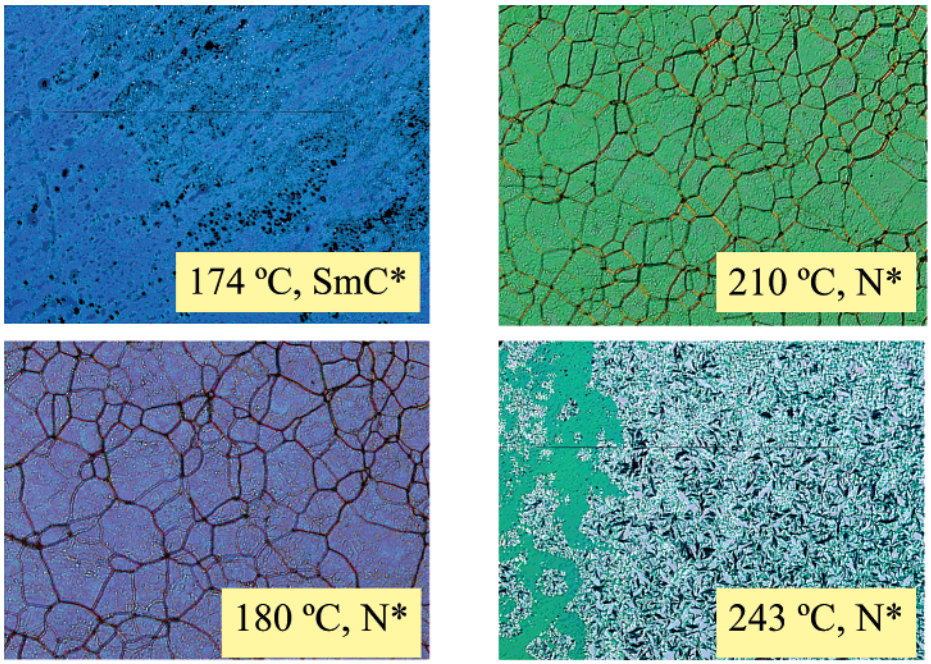

Figure 6. Polarizing microscope pictures (crossed polarizers, ×100) of **NC-DCT-p10*(S)** at different temperatures. Grandjean textures of the N* phase indicate a spontaneous orthogonal surface alignment of the helices (planar boundary conditions of the molecules), and the change of the iridescent color, a decrease in pitch with increasing temperature. On approaching the isotropic phase the alignment of the helices was lost, and a focal-conic texture appeared at 243 °C.

material to display an enantiotropic nematic mesophase. However, the suppression of liquid crystalline behavior is very strong, since doping of the nonchiral **NC-TCT-mp** derivatives with chiral molecules, chiral-liquid crystals, or the chiral **NC-TCT-mp** derivatives discussed previously all result in phase separation into an isotropic liquid phase and the nonchiral mesophase of the **NC-TCT-mp** derivative. Thus, mesophases of the **NC-TCT-mp** tetracatenars are not compatible with chiral induction, most likely due to unfavorable conformational changes.

In consideration of our hypothesis that steric repulsion originating from the chiral centers destabilized the mesophase, we investigated lowering the number of side chains and attaching chiral side chains to only one end of the molecule. Derivatives **NC-DCT-p10*(S)**, **NC-TrCT-mp4,p10*(S)**, and **NC-TrCT-mp6,p10*(S)** display SmC*- and N*-phases between 138° and 248 °C, while **NC-DCT-p4*(S)** displays a N*-phase and **NC-TCT-mp6,mp10*(R)** a SmC*-phase only (Schemes 1 and 2, Table 3). The N*-phases of **NC-DCT-p10*(S)**; **NC-TrCT-mp4,p10*(S)**; and **NC-TrCT-mp6,p10*(S)** displayed a pitch in the wavelength range of visible light as can be concluded from their iridescent Grandjean textures (Figure 6). The (complementary) color change of **NC-DCT-p10*(S)** from purple to green indicates a decrease in pitch with increasing temperature. Heating of the sample to temperatures above 240 °C, close to the clearing transition, resulted in a loss of the orthogonal surface alignment of the helices and appearance of a focal-conic texture.[41,42]

Preliminary electrooptical measurements on the SmC* of **NC-DCT-p10*(S)**; **NC-TrCT-mp6,p10*(S)**; and **NC-TCT-mp6,-mp10*(R)** are suggestive of ferroelectric behavior of the di- and tricatenars as well as possibly antiferroelectric behavior of the tetracatenar. Triangular wave measurements show evidence of switching, and we also observe a commensurate optical switching of the focal conic domains. However, large resistive currents, possibly due to ionic impurities that could not be removed, precluded detailed characterization of the ferroelectric and antiferroelectric behavior at this time. Future efforts will seek to resolve this issue.

Conclusions

Though bent cores and strong lateral dipoles typically disturb calamitic mesophases, we were able to demonstrate that combining both of these structural features can result in enantiotropic mesomorphism over wide temperature ranges. In fact, the phase diagram of the bent tetracatenars containing two lateral cyano groups at the central thiophene ring (**NC-TCT**) is very similar to what has been found for common straight-rod tetracatenars. We obtained nematic, smectic, columnar, and cubic mesophases by changing the length and substitution pattern of the four aliphatic side chains. At a molecular level, however, we propose distinct differences and explain the unusual behavior of the **NC-TCT** derivatives with an antiparallel dimer formation. The antiparallel dimer formation is incompatible with the formation of chiral mesophases. Only tetracatenars of lower symmetry and analogues with fewer side chains tolerated chiral induction, and chiral-nematic and SmC phases were obtained. Investigations of electrooptical properties of the chiral phases are the focus of our ongoing efforts.

Acknowledgment. We are grateful for the generous financial support from NEDO and the National Science Foundation. This work made use of equipment provided by the MRSEC Program

(41) Coles, H. in *Handbook of Liquid Crystals* Demus, D., Goodby, J., Gray, G. W., Spiess, H.-W., Vill, V., Eds.; Wiley−VCH: Weinheim, 1998; Vol. 1, p 343, 350, 365.
(42) Demus D.; Richter, L. In *Textures of Liquid Crystals*; 1st ed.; VEB Deutscher Verlag, fuer Grundstoffindustrie: Leipzig, 1978; pp 55−57.

of the National Science Foundation under award number DMR 98-08941

Supporting Information Available: Experimental details, characterization data and crystallographic information (PDF). This material is available free of charge via the Internet at http://pubs.acs.org.

JA0268027